Journal of Sensor Science and Technology
Vol. 33, No. 6 (2024) pp. 504-509
http://dx.doi.org/10.46670/JSST.2024.33.6.504
pISSN 1225-5475/eISSN 2093-7563

Highly Sensitive Platinum-Decorated Tungsten Oxide for Ultra-Low-Concentration Hydrogen Detection

Yuntae Ha[1,2], Dong Geon Jung[1], Junyeop Lee[1], Yijun Yang[1,2], Uksu Han[1,2], and Daewoong Jung[1,+]

Abstract

The global transition towards a hydrogen-based economy has increased the need for highly sensitive hydrogen gas sensors capable of detecting ultra-low concentrations. Although conventional hydrogen sensors have been widely studied and applied, they face fundamental limitations in terms of sensitivity, selectivity, and power consumption at low concentrations. Here, we report a high-performance hydrogen sensor based on platinum-decorated tungsten oxide (WO_3/Pt) fabricated using MEMS technology. The sensor was systematically constructed through the sequential processes of thermal oxidation, LPCVD, electrode patterning, and membrane formation. The WO_3/Pt composite, synthesized via a modified wet impregnation method and thoroughly characterized via XRD, demonstrated a uniform platinum distribution on the WO_3 surface. The fabricated sensor exhibited exceptional sensitivity across a hydrogen concentration range of 100–500 ppm with enhanced concentration resolution and reproducibility. Under optimal operating conditions at 300°C, the sensor achieved rapid response/recovery kinetics while maintaining a low power consumption of 42.1 mW. The enhanced sensing performance is attributed to the synergistic effects between WO_3 and the Pt catalyst, specifically the spillover effect and efficient modulation of the depletion layer at the Pt-WO_3 interface.

Keywords: Hydrogen, Gas sensor, Tungsten oxide, Low-concentration detection

1. INTRODUCTION

The global transition towards a hydrogen-based economy has increased the need for ultra-sensitive hydrogen detection technologies [1]. Owing to its high gravimetric energy density and zero-emission characteristics, hydrogen has emerged as a promising alternative energy carrier to address escalating climate change concerns [2]. This paradigm shift demands advanced sensing technologies capable of detecting ultra-low hydrogen concentrations for applications ranging from industrial processes to medical diagnostics [3].

Hydrogen sensors serve crucial functions in diverse fields, particularly in industrial process control, fuel-cell system monitoring, and medical diagnostics. In medical applications, ultra-low-concentration hydrogen sensors have shown promise as non-invasive diagnostic tools, especially for conditions such as irritable bowel syndrome (IBS) and gastrointestinal disorders [4]. These sensors enable the detection of trace amounts of hydrogen in exhaled breath, providing valuable insights into metabolic processes and gut health without the need for invasive procedures.

Among the various hydrogen sensing technologies, including electrochemical, catalytic, and metal oxide semiconductor (MOS) sensors [5], MOS-based sensors have attracted increased attention owing to their inherent advantages in terms of sensitivity, response time, and compatibility with microelectronic fabrication. Tungsten oxide (WO_3) has emerged as an exceptional sensing material, particularly for reducing gases such as hydrogen [6]. The sensing mechanism relies on surface oxygen chemisorption and subsequent interaction with the target gases, manifesting as measurable changes in electrical conductivity [7].

However, conventional sensing technologies face significant challenges in terms of key performance metrics. Current sensing technologies have fundamental limitations, including insufficient sensitivity at ultra-low concentrations, inadequate selectivity, delayed response times, and excessive power consumption [8]. Additionally, environmental factors and interfering gases can compromise the sensor accuracy, highlighting the need for more robust detection technologies.

[1] Korea Institute of Industrial Technology, KITECH
320, Techno sunhwan ro, Yuga-eup, Dalseong-gun, Daegu 42994, Korea
[2] School of Electronic and Electrical Engineering, Kyungpook National University
80, Daehak-ro, Buk-gu, Daegu 41566, Korea
[+]Corresponding author: dwjung@kitech.re.kr
(Received : Nov. 7, 2024, Revised : Nov. 12, 2024, Accepted : Nov. 15, 2024)

Recent advances in nanotechnology have introduced promising solutions by incorporating noble metal nanoparticles, such as platinum (Pt), into metal oxide sensing layers [9]. These particles enhance the sensor performance via catalytic activity and the spillover effect, in which dissociated hydrogen atoms migrate from the metal catalyst to the metal oxide surface [10]. Concurrently, micro-electro-mechanical systems (MEMS) technology has revolutionized sensor development by enabling miniaturization, reduced power consumption, and mass-production capabilities [11].

In this paper, we present a high-performance hydrogen sensor using MEMS technology and WO_3/Pt composites, targeting specific performance metrics, including a detection limit below 1 ppm, a response time under 10 s, and a recovery time of less than 30 s. Our approach aims to comprehensively address crucial challenges by optimizing the sensing layer structure, controlling the platinum distribution, and implementing efficient thermal management through a novel MEMS design. Advanced characterization techniques, including X-ray diffraction (XRD), were employed to reveal the structural and chemical properties of the sensing materials, while performance evaluation encompassed various operating conditions and potential interfering gases.

We also explored photoactivation to enhance the performance at lower operating temperatures, potentially improving the long-term stability of the system while reducing its power consumption [12]. This study aimed to make significant contributions to both the hydrogen energy and medical diagnostic fields, potentially revolutionizing environmental monitoring, industrial safety, and personalized medical treatment through next-generation gas-sensing technologies.

2. EXPERIMENTAL

2.1 WO_3/Pt composite synthesis

WO_3/Pt composites were synthesized using the optimized wet impregnation method [13]. Briefly, 1 g of WO_3 powder was dispersed in 10 mL of ethanol. Then, 0.01 g of hexachloroplatinic acid (H_2PtCl_6) was added to this dispersion as the Pt precursor. The resulting mixture was magnetically stirred for 90 min at room temperature. An organic vehicle was prepared by dissolving ethyl cellulose (0.5 g) in ethanol (8 mL), followed by the addition of 4 g of terpineol. This organic vehicle was then added to the WO_3/Pt precursor dispersion. The combined mixture was heated to 80°C while stirring for 60 min to promote Pt reduction and attachment to the WO_3 particles. After cooling to room temperature, the dispersion was further stirred for 48 h to ensure a complete reaction and uniform distribution of the Pt particles on the WO_3 surface. The resulting WO_3/Pt composite was collected via centrifugation, washed repeatedly with ethanol, and dried at 60°C overnight. The final product was a grey powder consisting of WO_3 particles decorated with a Pt catalyst.

2.2 Hydrogen gas sensor fabrication

The gas sensor was fabricated using conventional semiconductor processing techniques and systematic optimization. First, a 1-μm-thick thermal oxide layer was grown on a silicon wafer, followed by the low-pressure chemical vapor deposition (LPCVD) of a 300-nm Si_3N_4 layer. Titanium/platinum heaters and electrodes were patterned via photolithography and lift-off. A 300-nm SiO_2 passivation layer was deposited via plasma-enhanced chemical vapor deposition (PECVD). The heater and electrode regions were opened via reactive-ion etching (RIE) with CF_4/O_2 plasma. An oxide/nitride/oxide (O/N/O) stack was etched for membrane release. The membrane was released via XeF_2 etching to create a floating structure. The sensing material was drop-cast onto the membrane surface. Finally, the sensor was fabricated by sintering and annealing the sensing material film.

To deposit the sensing layer, the synthesized WO_3/Pt composite was dispersed in ethanol at a concentration of 10 mg/mL and sonicated for 30 min to ensure a uniform dispersion. A precise volume of 2 μL of this WO_3/Pt suspension was drop-cast onto the suspended membrane surface using a micropipette. The drop-casting was carefully positioned to cover the electrode area while maintaining a uniform thickness. After drop-casting, the device was sintered at 80°C for 2 h. Finally, the sensor was completed by

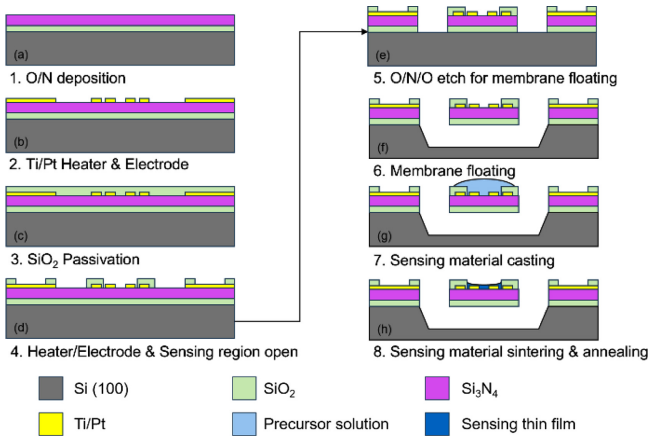

Fig. 1. Schematic of the hydrogen gas sensor fabrication process.

annealing at 300°C for 2 h in air to ensure good adhesion and crystallization of the sensing layer. This fabrication process, as shown in Fig. 1, resulted in a suspended membrane structure for thermal isolation with integrated heaters and electrodes, which was optimized for gas-sensing applications.

3. RESULTS AND DISCUSSION

3.1 WO_3/Pt composite characterization

The morphological and structural characteristics of the synthesized WO_3/Pt composite were investigated via XRD. The crystalline structure of the WO_3/Pt composite was also examined via XRD. For XRD characterization, the synthesized WO_3/Pt solution was spin-coated onto a silicon substrate (25 × 25 mm^2) at 1500 rpm for 30 s, followed by thermal annealing at 90°C for 30 min. As shown in Fig. 2, the XRD pattern exhibits well-defined diffraction peaks at 23.1°, 23.6°, and 24.4°, respectively corresponding to the (002), (020), and (200) planes of monoclinic WO_3. The less intense but distinguishable peaks at 39.8° and 46.2° are attributed to the (111) and (200) planes of metallic Pt, respectively, which is consistent with the low loading (2 wt%) of the noble metal catalyst.

3.2 Hydrogen detection characteristics

The thermal performance of the fabricated microheater was systematically evaluated before the gas-sensing measurements. The resistance of the temperature sensor was monitored in real-time by varying the chamber temperature from room temperature to above 300°C under controlled relative-humidity conditions, enabling precise characterization of the microheater's heating capabilities. The heating characteristics were analyzed by applying input voltages ranging from 0 to 4 V to the microheater, while simultaneously measuring the corresponding temperature

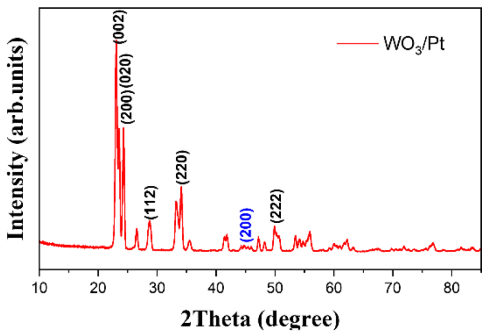

Fig. 2. XRD patterns of the WO_3/Pt composite after synthesizing

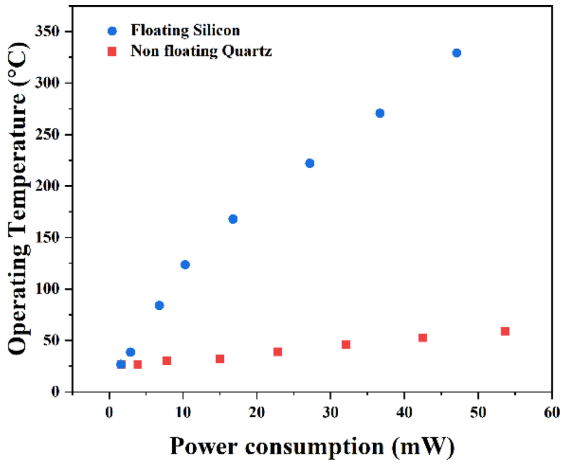

Fig. 3. Power consumption of the fabricated microheater according to the operating temperature.

sensor resistance changes across the operating temperature range.

The experimental results revealed that while the power consumption increased proportionally with the heater line width, the heating performance per unit power consumption exhibited no significant variation across different linewidths at equivalent operating temperatures, as shown in Fig. 3. This behavior can be primarily attributed to the Joule heating effect, where the thermal performance is predominantly determined by the current flow through the heater structure. The relatively small linewidth variations did not substantially affect the thermal generation characteristics within the same structural configuration, maintaining consistent temperature profiles across the sensing area. The temperature ramping characteristics exhibited a linear behavior with the applied voltage, demonstrating reliable temperature control beyond 300°C at 4 V with minimal thermal hysteresis. These findings suggest that further microheater performance enhancements would require optimization through novel geometric designs rather than simple linewidth adjustments to improve the power efficiency and temperature uniformity.

The operating temperature was derived from the relationship between the temperature sensor measured resistance and temperature, while the power consumption (P, in W) was calculated as follows:

$$P = \frac{V^2}{R}, \tag{1}$$

where P is the power consumption (W), V is the applied voltage (V), and R is the microheater resistance (Ω).

The WO_3/Pt-based hydrogen gas sensor exhibited optimal performance at an operating temperature of approximately 300°C, with a corresponding power consumption of 42.1 mW. At this

optimized temperature, the sensor response characteristics were systematically evaluated by exposing them to hydrogen gas at concentrations ranging from 100 to 500 ppm. The measurements were conducted under a constant total gas flow rate of 1000 sccm with response and recovery times of 5 min each to ensure stable and reproducible measurements.

To evaluate the gas-sensing characteristics of the fabricated WO_3/Pt-based hydrogen gas sensor, measurements were performed in a controlled gas chamber environment. Sensing measurements were performed using a Source Meter Unit (SMU, B2902A, Keysight), with voltages of 3.5 and 3 V applied to the microheater and sensing electrodes, respectively. As shown in Fig. 4, the sensor exhibits a sustainable concentration resolution and remarkably high response characteristics across a hydrogen detection range of 100-500 ppm. As shown Fig. 5, the fabricated WO_3/Pt-based hydrogen sensor exhibits a stable response to a hydrogen concentration of 500 ppm. These findings demonstrate the reliable cyclic stability of the fabricated sensor for practical applications.

Additionally, the selectivity of the WO_3/Pt composite sensor to other interfering gases was systematically evaluated. In addition to H_2, various potential interfering gases, including CO_2, CO, and C_2H_2, were tested with the sensor at the optimal operating temperature (300°C). The selectivity results for each gas are shown in Fig. 6. Although the sensor exhibited a robust response of 94% to H_2, the responses to interfering gases at the same concentration (500 ppm) were significantly lower, all below 2%. This exceptional selectivity towards hydrogen can be attributed to the synergistic effect between the WO_3 and Pt particles at the heterojunction interface [14]. The Pt catalyst preferentially promotes hydrogen molecule dissociation via the spillover effect, while the optimized operating temperature of 300°C provides ideal conditions for hydrogen-specific catalytic reactions. These combined effects resulted in a substantially higher sensitivity to

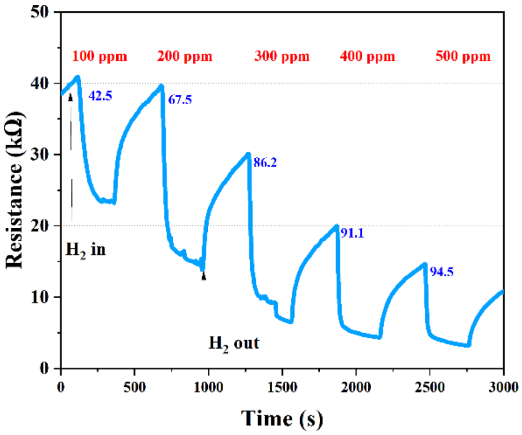

Fig. 4. Measured output resistance of the WO_3/Pt-based H_2 gas sensor with microheaters.

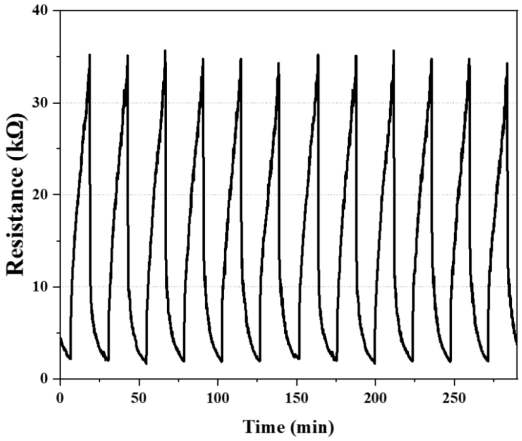

Fig. 5. Repeatability of the WO_3/Pt-based gas sensor at a hydrogen concentration of 500 ppm.

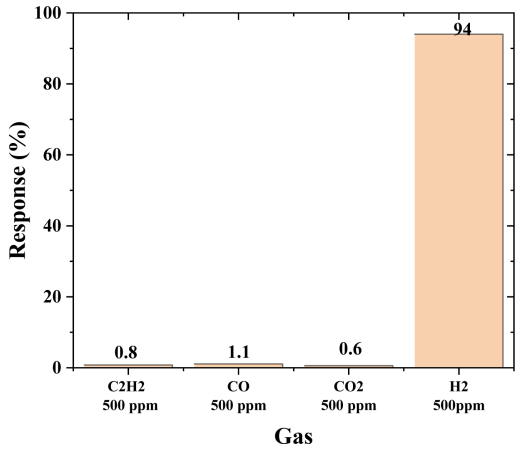

Fig. 6. Selectivity of the WO_3/Pt-based gas sensor towards 500 ppm of the target gases at 300°C.

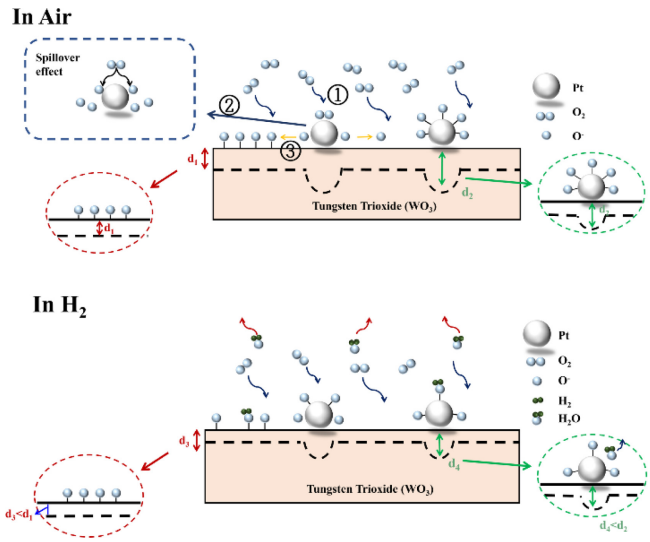

Fig. 7. Hydrogen sensing mechanism of the Pt/WO_3 composite.

hydrogen than to other interfering gases, demonstrating the practical viability of our WO_3/Pt composite sensor for selective hydrogen detection.

As shown in Fig. 7, the sensing mechanism relies primarily on the interplay between the semiconductor surface redox reactions and charge carrier dynamics [15]. Initially, atmospheric oxygen molecules undergo chemisorption at the WO_3/Pt interface. Through the spillover effect facilitated by the Pt catalyst, dissociated oxygen species capture electrons from the WO_3 conduction band, becoming ionized ($O_2 + 2e^- \rightarrow 2O^-$) [16]. This charge transfer mechanism generates an electron-depletion layer on the WO_3 surface, which significantly reduces electrical conductivity.

Upon exposure to hydrogen gas, hydrogen molecules activated at the Pt catalyst surface undergo an oxidation-reduction reaction with chemisorbed oxygen ions, forming H_2O ($H_2 + 2O^- \rightarrow H_2O + 2e^-$). The electrons released during this process are reinjected into the WO_3 conduction band, reducing the electron-depletion layer width and lowering the potential barriers between the grain boundaries, thereby increasing the electrical conductivity. The magnitude of the conductivity change is proportional to the H_2 partial pressure, forming the basis for quantitative gas detection.

The Pt catalyst introduced in this study enhanced the electronic properties of the WO_3 interface. The Pt catalytic activity significantly accelerates oxygen dissociative adsorption and hydrogen oxidation reactions, while the increased electron mobility at the Pt/WO_3 heterojunction interface enhances the gas-sensing characteristics. This interfacial charge transfer mechanism facilitates the effective modulation of the depletion layer and induces dramatic changes in the potential barrier height, leading to enhanced sensitivity. Consequently, incorporating a Pt catalyst enhances the WO_3 electronic properties, which play a crucial role in achieving improved sensitivity and selectivity within the operating temperature range.

4. CONCLUSIONS

In this study, we developed a high-performance gas sensor based on platinum-decorated tungsten oxide (WO_3/Pt) for ultra-sensitive hydrogen detection. The WO_3/Pt composite was synthesized via the wet impregnation method and characterized via XRD. The XRD analysis results revealed characteristic diffraction peaks for both the WO_3 crystal structure and Pt nanoparticles. The sensor platform, fabricated via MEMS processing, employed a suspended membrane structure for thermal stability and low power consumption. The microheater performance evaluation results revealed a low power consumption of 42.1 mW at an operating temperature of 300°C, exhibiting significantly improved power efficiency compared to conventional bulk-type sensors.

Gas-sensing characterization revealed excellent linearity and sensitivity across hydrogen concentrations ranging from 100 to 500 ppm. Notably, the sensor exhibited a high sensitivity of 42.5%, even at a low hydrogen concentration of 100 ppm, with a sensitivity of up to 94.5% at higher concentrations. These enhanced sensing characteristics can be attributed to the catalytic effect of the Pt nanoparticles and efficient charge transfer at the WO_3/Pt heterojunction interface. The sensing mechanism was based on the electron depletion layer modulation through oxygen ion formation at the WO_3/Pt interface and subsequent redox reactions with hydrogen molecules. Particularly, the spillover effect of Pt nanoparticles promotes hydrogen molecule dissociation and reactivity, substantially enhancing the sensor's sensitivity and selectivity. Repeated measurements confirmed the sensor's excellent reproducibility and stability. Furthermore, the results demonstrate that our WO_3/Pt-based MEMS sensor has great potential as a high-performance, low-concentration hydrogen detection system, as required for the emerging hydrogen economy. We anticipate that further improvements in the detection limits and stability evaluations under various environmental conditions would enhance its practical applicability. Moreover, the sensor platform developed in this study shows promise for the detection of other gas species.

ACKNOWLEDGEMENTS

This study was conducted with the support of the Korea Institute of Industrial Technology for the development of an artificial intelligence-based hydrogen sensor to ensure fuel cell vehicle safety in real driving environments (Kitech UR-24-0028).

This work was supported by the Korea Innovation Foundation (INNOPOLIS) grant funded by the Korean government; (MSIT) (2020-DD-UP-0348).

REFERENCES

[1] G. Pandey, H. M. Lee, T. H. Kim, and Y. B. Kim, "Synergistic effects of Pd-Ag decoration on SnO/SnO_2 nanosheets for enhanced hydrogen sensing", *Sens. Actuators B Chem.*, Vol. 402, p. 135062, 2024.

[2] International Energy Agency, *The Future of Hydrogen*, IEA, Paris, 2019.
[3] X. Chen, R. Liu, Y. Wang, and H. Wu, "Nanostructured gas sensors: From air quality and environmental monitoring to healthcare and medical applications", *Nanomaterials*, Vol. 11, No. 8, p. 1927, 2021.
[4] M. Ledochowski, B. Widner, C. Murr, B. Sperner-Unterweger, and D. Fuchs, "Fructose malabsorption is associated with decreased plasma tryptophan", *Scandinavian J. Gastroenterol.*, Vol. 36, No. 4, pp. 367-371, 2001.
[5] T. Hübert, L. Boon-Brett, G. Black, and U. Banach, "Hydrogen sensors - A review", *Sens. Actuators B Chem.*, Vol. 157, No. 2, pp. 329-352, 2011.
[6] M. G. Chung, H. M. Lee, T. Kim, J. H. Choi, D. k. Seo, J. B. Yoo, S. H. Hong, T. J. Kang, and Y. H. Kim, "Highly sensitive NO_2 gas sensor based on ozone treated graphene", *Sens. Actuators B Chem.*, Vol. 166, pp. 172-176, 2012.
[7] C. Wang, L. Yin, L. Zhang, D. Xiang, and R. Gao, "Metal Oxide Gas Sensors: Sensitivity and Influencing Factors", *Sensors*, Vol. 10, No. 3, pp. 2088-2106, 2010.
[8] G. Korotcenkov, "Metal oxides for solid-state gas sensors: What determines our choice?", *Mater. Sci. Eng. B*, Vol. 139, No. 1, pp. 1-23, 2007.
[9] N. Yamazoe, G. Sakai, and K. Shimanoe, "Oxide semiconductor gas sensors", *Catal. Surv. Asia*, Vol. 7, No. 1, pp. 63-75, 2003.
[10] P. J. Kelly and R. D. Arnell, "Magnetron sputtering: a review of recent developments and applications", *Vacuum*, Vol. 56, No. 3, pp. 159-172, 2000.
[11] Z. Yuan, F. Yang, F. Meng, K. Zuo, and J. Li, "Research of low-power MEMS-based micro hotplates gas sensor: A Review", *IEEE Sens. J.*, Vol. 21, No. 17, pp. 18368-18380, 2021.
[12] E. Comini, G. Faglia, and G. Sberveglieri, "UV light activation of tin oxide thin films for NO_2 sensing at low temperatures", *Sens. Actuators B Chem.*, Vol. 78, No. 1-3, pp. 73-77, 2001.
[13] T. Samerjai, C. Liewhiran, A. Wisitsoraat, A. Tuantranont, C. Khanta, and S. Phanichphant, "Highly selective hydrogen sensing of Pt-loaded WO_3 synthesized by hydrothermal/impregnation methods", *Int. J. Hydrogen Energy*, Vol. 39, No. 11, pp. 6120-6128, 2014.
[14] A. Boudiba, P. Roussel, C. Zhang, M. G. Olivier, R. Snyders, and M. Debliquy, "Sensing mechanism of hydrogen sensors based on palladium-loaded tungsten oxide (Pd-WO_3)", *Sens. Actuators B Chem.*, Vol. 187, pp. 84-93, 2013.
[15] C. H. Chang, T. C. Chou, W. C. Chen, J. S. Niu, K. W. Lin, S. Y. Cheng, J. H. Tsai, and W. C. Liu, "Study of a WO_3 thin film based hydrogen gas sensor decorated with platinum nanoparticles", *Sens. Actuators B Chem.*, Vol. 317, p. 128145, 2020.
[16] R. J. Bose, N. Illyaskutty, K. S. Tan, R. S. Rawat, M. V. Matham, H. Kohler, and V. P. M. Pillai, "Hydrogen sensors based on Pt-loaded WO_3 sensing layers", *Europhys. Lett.*, Vol. 114, No. 6, p. 66002, 2016.